Temperature and Pressure Dependent Rate Coefficients for the Reaction of Hg with Br and the Reaction of Br with Br: A Pulsed Laser Photolysis-Pulsed Laser Induced Fluorescence Study†

Deanna L. Donohoue, Dieter Bauer, Brandi Cossairt, and Anthony J. Hynes*

Division of Marine and Atmospheric Chemistry, Rosenstiel School of Marine and Atmospheric Science, University of Miami, 4600 Rickenbacker Causeway, Miami, Florida 33149

Received: August 19, 2005; In Final Form: November 29, 2005

A pulsed laser photolysis-pulsed laser induced fluorescence technique has been employed to study the recombination of mercury and bromine atoms, Hg + Br + M → HgBr + M (1) and the self-reaction of bromine atoms, Br + Br + M → Br_2 + M (2). Rate coefficients were determined as a function of pressure (200−600 Torr) and temperature (243−293 K) in nitrogen buffer gas and as a function of pressure (200−600 Torr) in helium buffer gas at room temperature. For reaction 1, kinetic measurements were performed under conditions in which bromine atoms were the reactant in excess concentration while simultaneously monitoring the concentration of both mercury and bromine. A temperature dependent expression of $(1.46 \pm 0.34) \times 10^{-32} \times (T/298)^{-(1.86\pm1.49)}$ cm^6 $molecule^{-2}$ s^{-1} was determined for the third-order recombination rate coefficient in nitrogen buffer gas. The effective second-order rate coefficient for reaction 1 under atmospheric conditions is a factor of 9 smaller than previously determined in a recently published relative rate study. For reaction 2 we obtain a temperature dependent expression of $(4.31 \pm 0.21) \times 10^{-33} \times (T/298)^{-(2.77\pm0.30)}$ cm^6 $molecule^{-2}$ s^{-1} for the third-order recombination rate coefficient in nitrogen buffer gas. The rate coefficients are reported with a 2σ error of precision only; however, due to the uncertainty in the determination of absolute bromine atom concentrations and other unidentified systematic errors we conservatively estimate an uncertainty of ±50% in the rate coefficients. For both reactions the observed pressure, temperature and buffer gas dependencies are consistent with the expected behavior for three-body recombination.

Introduction

In the atmosphere mercury exists primarily in its elemental form, Hg(0), which until recently was thought to be unreactive in the gas phase. Hg(0) is insoluble in water and has a low deposition rate. Estimates of the atmospheric lifetime of Hg(0) vary, but it is believed to be in the range of six months to one year. Mercury is a known toxin, and over the past decade there have been observations of increased mercury levels in Arctic lake waters,[1] Arctic animal populations,[2] and Arctic indigenous human populations.[3] With no known local sources of mercury and no known physical or chemical process that could concentrate mercury in the Arctic, these high levels of mercury were an enigma and a significant health concern. Recent observations in polar regions suggest that under certain conditions, probably as a result of reaction with halogens, Hg(0) can be rapidly oxidized to a form which has a much higher deposition rate. Thus interest in understanding the detailed mechanism of atmospheric mercury transformation has grown.

The first direct evidence of a fast atmospheric transformation of Hg(0) was observed in Alert Canada. In 1995, Schroeder et al.[4] conducted continuous surface-level measurements of total gaseous mercury. They discovered that with polar sunrise, there were frequent episodic events in which total gaseous mercury was almost completely depleted from the surface air. During these depletion events, a very strong correlation between the depletion of Hg(0) and ozone was observed. Following this initial study Atmospheric Mercury Depletion Episodes (AMDEs) have been observed in the Arctic,[4,5] Antarctic,[6,7] Greenland[8] and Norway.[9] The observations of AMDEs suggest that, at least under certain circumstances, mercury can undergo fast atmospheric transformations.

AMDEs seem to correlate well with tropospheric ozone depletion. Dramatic episodic depletions in tropospheric ozone have been recorded in polar regions over the last several years. Typically, these events take place in the spring after polar sunrise and can result in a reduction of ozone concentrations from 40 ppb to less than 1 ppb over the course of a single 24 h period. Early measurements[10] revealed a large increase in the levels of filterable bromine compounds that coincided with the ozone depletion events. Direct spectroscopic observations have shown that large increases in bromine monoxide, BrO, concentrations coincide with these depletion events; it seems clear that a catalytic cycle involving BrO plays a role in these ozone depletion episodes.[11] It is reasonable to suspect that similar halogen chemistry is driving AMDEs. The reactions of Hg(0) with BrO and Br have been suggested as a potential mechanism. However, there are few kinetic data available for rate coefficients of elemental mercury with halogen radicals, making it difficult to model AMDEs.

Additionally, there is evidence that an unknown gas-phase oxidation process influences concentrations of mercury in the marine boundary layer.[12,13] In a recent modeling study Hedgecock and co-workers[13] suggested that Br atoms are the primary oxidant of Hg(0) in the marine boundary layer and they calculate a typical lifetime of about 10 days. The implications of this for

† Part of the special issue "David M. Golden Festschrift".

10.1021/jp054688j CCC: $33.50
Published on Web 02/08/2006

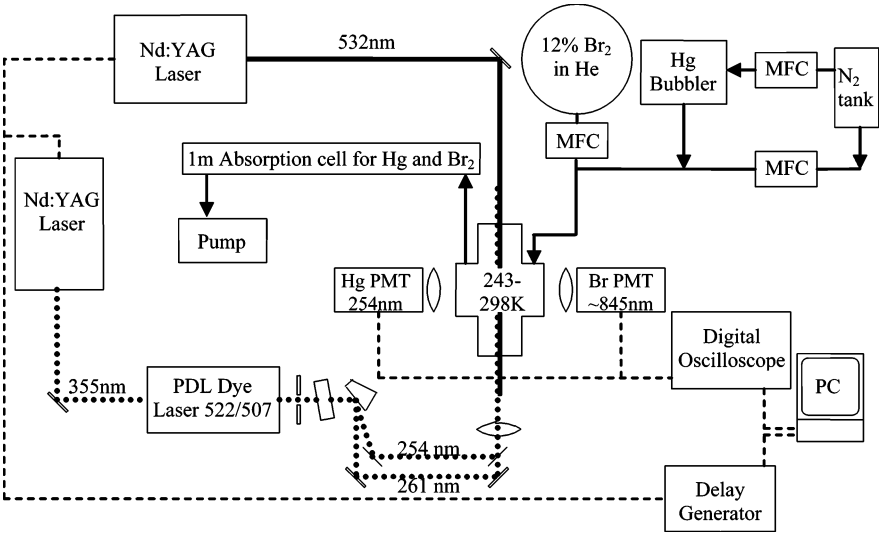

Figure 1. Experimental setup for the PLP−PLIF system to detect Hg atoms by one-photon LIF and Br atoms by two-photon LIF, including optical and flow system configurations.

chemistry on a global scale are unclear; because the precise mechanism of mercury transformation is unknown.

In an effort to elucidate the role of Br atoms in AMDEs and in the MBL, we have made direct measurements of the rate coefficient for the reaction of elemental mercury with bromine atoms, reaction 1, as a function of temperature and pressure in

$$\mathrm{Hg + Br + M \rightarrow HgBr + M} \qquad (1)$$

nitrogen and helium buffer gases. Kinetic measurements were performed with bromine as the reactant in excess concentration, while temporal profiles of both reactants were monitored by LIF. These measurements require an accurate determination of the Br atom concentration; thus we must account for the loss of Br atoms by the bromine atom recombination. Consequently, we also measured the rate coefficient for the recombination of bromine atoms, reaction 2, under similar experimental conditions. Reaction 2 has been studied several times before;[14−19] the results from this study will be compared to the previous results below.

$$\mathrm{Br + Br + M \rightarrow Br_2 + M} \qquad (2)$$

There have been three prior experimental[20−22] and two theoretical determinations[23,24] of the rate coefficient for reaction 1. We report rate coefficients that are significantly smaller than that in a recently published relative rate study,[21] but in reasonable agreement with the two previous theoretical determinations. An additional unpublished relative rate determination[22] reported two rate coefficients for two different reference molecules. The preferred value in that study was significantly faster than the rate reported in this work. However, the second rate coefficient reported in that study is in good agreement with the one in this work.

Experimental Section

The reaction between gaseous elemental mercury and bromine atoms was studied by pulsed laser photolysis−pulsed laser induced fluorescence (PLP−PLIF) as a function of pressure and temperature in nitrogen and helium buffer gas. Experiments were conducted at three temperatures, 293, 263 and 243 K, and three pressures, 200, 400 and 600 Torr. The experimental design is similar to the apparatus employed in the previously reported determination of the rate coefficient for mercury with chlorine atoms.[25]

Bromine atoms were produced by pulsed laser photolysis (PLP) of molecular bromine. The temporal profiles of both bromine atoms and mercury atoms were monitored by two- and one-photon laser induced fluorescence (LIF), respectively. The experimental configuration is detailed in Figure 1. The experiments were conducted in a temperature controlled Pyrex reaction vessel. Four mutually perpendicular sidearms with quartz windows were attached to the center of the vessel. The photolysis and the probe lasers were overlapped using dichroic mirrors and then propagated through two of the cell's sidearms, perpendicular to the gas flow. The temperature of the reaction vessel was controlled by a circulating methanol bath while the windows were constantly flushed with dry air to prevent condensation. A thermocouple was inserted into the reaction zone through a vacuum seal, allowing measurement of the gas temperature under the precise pressure and flow conditions of the experiment. Experiments were carried out under "slow-flow" conditions. The gas velocity was maintained at approximately 26 cm s^{-1}, to completely replace the gas mixture in the reaction zone between the laser pulses. All flows were monitored using calibrated mass flow controllers. The pressure in the reaction cell was monitored with a capacitance manometer.

Bromine atoms were produced by photolysis of molecular bromine using the 532 nm, third harmonic of a Nd:YAG laser.

$$\mathrm{Br_2} + h\nu \rightarrow \mathrm{Br + Br} \qquad (3)$$

An output power of approximately 500 mJ per pulse resulted in bromine atom concentrations ranging from 2.5×10^{15} to 40×10^{15} molecules cm^{-3}. The photolysis of molecular bromine at 532 nm from the $^3\Pi_{1u}$ and $^2\Pi_{0u+}$ bonding states to the $^1\Pi_{1u}$ repulsive exited state leads to the formation of two bromine atoms. Some of the resulting bromine atoms were electronically excited; however, these excited species were rapidly deactivated to the $^2P^0_{3/2}$ ground state,[26] resulting in a quantum yield for the photolysis of molecular bromine[19] of 2.

The buffer gas flowed through a mercury bubbler at room temperature. This produced stable mercury concentrations, which ranged from 5×10^{11} to 20×10^{11} molecules cm^{-3} under our flow conditions.

Elemental mercury and molecular bromine concentrations were monitored in situ by UV photometry using the 253.7 and 365 nm lines from a mercury lamp, respectively. The reaction mixture was passed through an absorption cell and the lamp output was split with a dichroic beam splitter and detected by two interference filter/photomultiplier (PMT) combinations and each absorbance was recorded. The molecular bromine concentrations were determined using a 1 m cell and the literature cross-section of molecular bromine[27] at 365 nm of 1.258×10^{-19} cm^2. The line width of the mercury absorption line is narrower than the broadened output of the mercury lamp; therefore, the cross-section depends on the line width of the lamp and requires a determination of the effective absorption cross-section. The effective cross-section of mercury determined in this system was 1.36×10^{-14} cm^2 for absorbencies less than 0.7, whereas a polynomial relationship was used for absorbencies greater than 0.7. The methods used to determine this cross-section and the relevant plot have been previously reported.[25] During kinetic measurements an absorption path length of 100 cm was used.

When both mercury and bromine were passed through the absorption cell, a significant reduction of the mercury concentration was observed, and the bromine concentration was left unchanged. This observation was expected because the bromine concentration was 3 orders of magnitude larger than the mercury concentration. These observations indicate that there is a heterogeneous reaction occurring within the system, most likely on the walls of the cell. Therefore, to reduce the affects of this heterogeneous chemistry, the absorption cell was placed after the LIF cell and the mercury and bromine gases were mixed immediately before the LIF cell. By reducing the mixing time and cell wall surface area before the detection zone, this loss of mercury was minimized.

The initial bromine atom concentration produced by photolysis was determined from[28]

$$[\mathrm{Br}] = [\mathrm{Br_2}]\cdot \mathrm{QY}\cdot(1 - \exp^{-(P_L/h)(c/\lambda)(\sigma_{Br2}/A_L)}) \qquad \text{(I)}$$

where QY is the quantum yield of reaction 3, P_L is the in laser power in joules, h is Planck's constant, c is the speed of light in cm s^{-1}, σ_{Br_2} is the absorbance cross-section at 532 nm in cm^2, λ is the laser wavelength in cm, and A_L is the area of the laser in cm^2. The photolysis laser has a nominally Gaussian profile; hence the beam passed through a ceramic aperture, located 2 m from the reaction zone, to cut off the edges of the beam. The variation in the fluence across the beam profile at the reaction zone was determined by measuring the power passing through a 0.05 cm pinhole ceramic aperture. The power meter/aperture combination was placed on a linear translation stage and the transmitted photolysis laser power was recorded in 0.05 cm steps giving the power variation across the horizontal diameter of the beam. From the observed beam profile the effective laser diameter in the reaction volume was determined to be 0.6 ± 0.05 cm. Over this diameter the beam profile has an approximately homogeneous or "top hat" power profile with a maximum deviation of $\pm$20% from the mean. The homogeneity of the beam was confirmed by evaluating the difference between laser power measurements conducted with and without an additional 0.487 cm aperture, which was located approximately 40 cm from the reaction zone. The ratio of the powers was in good agreement with that calculated from the ratio of the areas, suggesting that there are no significant hot spots in the center of the beam. The laser power was measured before and after the LIF cell for each decay. This was done to account for reflection loss on the windows, the small absorption of the laser before reaching the detection volume, and any variation in the laser power. The averaged laser power was used for the calculation of the bromine atom production.

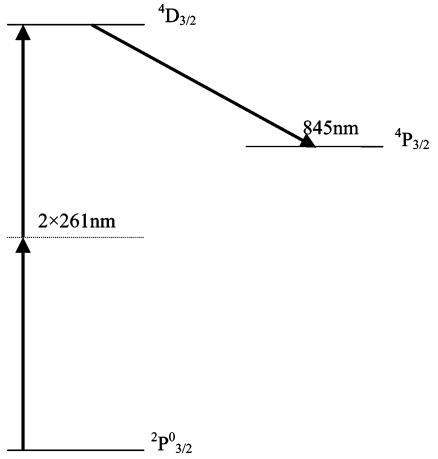

Figure 2. Excitation scheme for the two-photon LIF of Br atoms. The excitation transition is at 2×261 nm with the subsequent fluorescence transition near 845 nm.

Fluorescence was detected by two PMTs positioned perpendicular to both the direction of propagation of the laser beams and the direction of the gas flow. The PMT signals were typically averaged for 50 laser pulses by a 500 MHz digital scope and logged on a computer. The temporal profiles of the LIF signals were then constructed by varying the delay time between the photolysis and probe lasers using a digital delay generator.

Br Atom LIF Detection. The relative Br atom concentration was monitored by a two-photon LIF excitation scheme described previously in the literature.[29] This excitation scheme involves the two-photon excitation of the spin forbidden 5p $^4D^0_{3/2}-4p^5\ ^2P^0_{3/2}$ transition near 261 nm with subsequent fluorescence detection near 855 nm from the 5p $^4D^0_{3/2}-5s\ ^4P_{5/2}$ transition, as shown in Figure 2. The 261 nm probe laser, with typical output powers in the range 85−300 μJ, was generated by frequency doubling the 522 nm output from a tunable dye laser (Spectra Physics PDL3). The fluorescence was detected by a PMT with both an interference filter centered at 850 nm and a 750 nm cutoff filter to eliminate laser stray light. A 60 cm focal length lens was used to focus the laser beam into the detection volume, resulting in a detection limit of 2.0×10^{13} molecules cm^{-3} for measurements in high pressures of nitrogen.

Hg Atom LIF Detection. The relative Hg concentration was monitored by exciting the 6p $^3P^0_1-6s^2\ ^1S_0$ transition at 253.7 nm. The excitation beam was generated by frequency doubling the 507 nm output of a dye laser (Spectra Physics PDL3), which was then passed through a variable attenuator and reduced to a laser power of approximately 5 μJ, to avoid saturation of the 6p $^3P^0_1-6s^2\ ^1S_0$ transition, and thus reduce the laser stray light. Resonance fluorescence was observed by a PMT with an interference filter centered at 254 nm. A lens was used to adjust the diameter of the probe beam to about 0.3 cm, approximately half the size of the photolysis laser. This size was found to give best results for the detection of mercury while minimizing diffusion related problems. For the mercury LIF the detection limit was less than 4×10^{10} molecules cm^{-3} for low-pressure helium measurements and 2×10^{11} molecules cm^{-3} for measurements conducted in high pressures of nitrogen.

Results

Measurements of Hg + Br + M → HgBr + M (M = He, N_2). Direct determination of rate coefficients for the reactions

of gaseous elemental mercury presents a significant experimental challenge due to the low vapor pressure of mercury. The low vapor pressure makes it difficult to study the kinetics of this system using a traditional approach with the stable reactant in pseudo-first-order excess for anything other than reactions with very fast rate coefficients. To overcome these difficulties, we made kinetic measurements under conditions in which bromine atoms were the reactant in excess while simultaneously monitoring the concentration of both reactants.

The rate coefficient for the recombination of mercury and bromine atoms, reaction 1, was determined with Br atom concentrations typically 5000 times larger than the mercury concentration. Both mercury and bromine atom concentrations were monitored by LIF. The Br atom concentration was varied between 2.5×10^{15} and 40×10^{15} molecules cm^{-3}, and Hg concentrations were in the range $(5-20) \times 10^{11}$ molecules cm^{-3}.

At the Br atom concentrations required to observe a significant loss of mercury atoms, the bromine atom recombination reaction, reaction 2, resulted in a significant decrease in Br atom concentration on the time scale of the mercury atom decays. Because the Br atom concentration was not constant, a simple pseudo-first-order decay, i.e., an exponential decay, of mercury atoms was not observed. Instead, the mercury temporal profiles were fit by numerical integration, and the observed bromine temporal profiles were analyzed assuming simple second-order kinetics.

The temporal profiles of the bromine and mercury atoms were characterized by

$$\frac{d[Hg]}{dt} = -k_1[Br][Hg][M] \qquad (II)$$

$$\frac{d[Br]}{dt} = -2k_2[Br]^2[M] - k_1[Br][Hg][M] \qquad (III)$$

Because the concentration of mercury was at least 3 orders of magnitude smaller than the initial Br atom concentration, $k_1[Hg]$ should be at least 1 order of magnitude smaller than $k_2[Br]$; therefore, the second term in eq III is negligible and results in the simplified equation

$$\frac{d[Br]}{dt} = -2k_2[Br]^2[M] \qquad (IV)$$

For each experimental condition, temporal profiles of bromine and mercury atoms were measured using LIF. Typical sets of temporal profiles of each atom are shown in Figures 3 and 4. Under each set of conditions, i.e., a fixed pressure, temperature and initial bromine atom concentration, the effective second-order rate coefficient, k_2', for the recombination of bromine atoms was calculated from

$$\frac{1}{[Br]_t} = 2k_2't + \frac{1}{[Br]_0} \qquad (V)$$

which assumes that first-order losses by diffusion and reaction with impurities are negligible. Substituting [Br] into eq II gives

$$\frac{d[Hg]}{dt} = -k_1'[Hg]\left(\frac{1}{2k_2't + (1/[Br]_0)}\right) \qquad (VI)$$

This equation was numerically integrated to give the best fit to the measured mercury profiles and hence a value for k_1', the effective second-order rate coefficient for the recombination of Hg with Br. The numerical integration procedure was checked

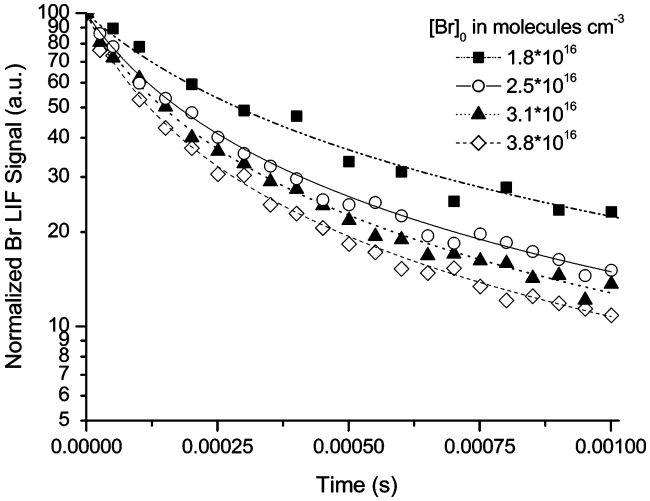

Figure 3. Typical bromine atom temporal profiles, shown for measurements conducted in 400 Torr N_2 at 243 K.

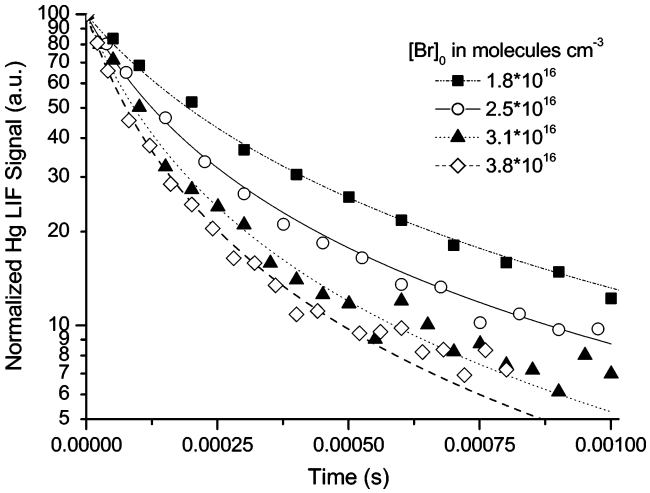

Figure 4. Typical mercury atom temporal profiles, shown for measurements conducted in 400 Torr N_2 at 243 K.

by simulating the measured decays using the derived values of k_1' and k_2' in the ACUCHEM program.[30]

The numerically integrated fits to the observed mercury temporal profiles are shown as lines in Figure 4 and the second-order rate coefficients, k_1', obtained in He and N_2 are listed in Table 1. Molecular nitrogen quenched the mercury fluorescence signal efficiently; therefore, the fluorescence yield and thus the S/N ratio degraded with increasing pressure. This was most noticeable in the 243 K dataset; however, the overall accuracy of the pressure dependent rate data should not have been significantly affected by this reduction of the S/N ratio.

The third-order recombination rate coefficients were then determined from linear fits of the plots of the second-order rate coefficients, k_1', versus the concentration of N_2 or He, as shown in Figure 5. The plots show the expected linear dependence of rate coefficient versus concentration, indicating that the reaction was in the low pressure, third-order regime, as might be expected for an atom−atom recombination. Assuming that the recombination rate coefficients are in the low pressure limit, the effective second-order rate coefficient should be zero at zero pressure. Consequently, the third-order recombination rate coefficients, k_1, have been calculated by forcing the plots through the origin. The difference between the forced and unforced slopes was under 7% and within the precision of the fit. The third-order recombination rate coefficients, k_1, are listed in Table 2 and

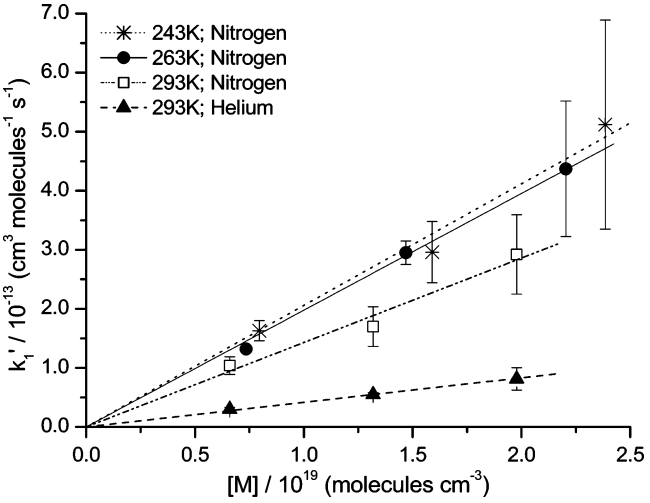

Figure 5. Variation of the effective second-order rate coefficients for the recombination Hg and Br atoms, k_1', with pressure.

TABLE 1: Second-Order Rate Coefficients for the Recombination of Mercury and Bromine Atoms, k_1'

gas	T (K)	P (Torr)	$10^{13}(k_1' \pm 2\sigma$ error) (cm^3 $molecule^{-1}$ s^{-1})
N_2	243	200	1.63 ± 0.17
		400	2.96 ± 0.52
		600	5.12 ± 1.77
	263	200	1.32 ± 0.05
		400	2.95 ± 0.20
		600	4.37 ± 1.15
	293	200	1.04 ± 0.15
		400	1.70 ± 0.34
		600	2.92 ± 0.67
He	293	200	0.30 ± 0.03
		400	0.55 ± 0.03
		600	0.81 ± 0.19

TABLE 2: Third-Order Rate Coefficients for the Recombination of Mercury and Bromine Atoms, k_1, Determined in This Work at 293 K in He and 243, 263, and 293 K in N_2, with the Resulting Temperature Dependent Expression for N_2

gas	T (K)	$10^{32}(k_1 \pm 2\sigma$ error) (cm^6 $molecule^{-2}$ s^{-1})
He	293	0.42 ± 0.02
N_2	243	2.06 ± 0.18
	263	1.98 ± 0.07
	293	1.43 ± 0.13
		$(1.46 \pm 0.34) \times 10^{-32} \times (T/298)^{-(1.86\pm1.49)}$

plotted in Figure 6. The temperature dependent expression for reaction 1 in nitrogen is given by eq VII reported with 2σ errors

$$k_{1,N_2}(243-298\text{K}) = (1.46 \pm 0.34) \times 10^{-32} \times \left(\frac{T}{298}\right)^{-(1.86\pm1.49)} \quad \text{(VII)}$$

of precision only. However, due to uncertainty in the calculation of absolute Br atom concentrations, which is discussed below, and other unidentified systematic errors, we conservatively estimate the error in the rate coefficient to be ±50%. The observed behavior is consistent with a three-body recombination, demonstrating a positive pressure dependence, an inverse temperature dependence, and a slower rate coefficient in helium than in nitrogen.

Measurements of Br + Br + M → Br_2 + M (M = He, N_2). The determination of temporal profiles of Br atom

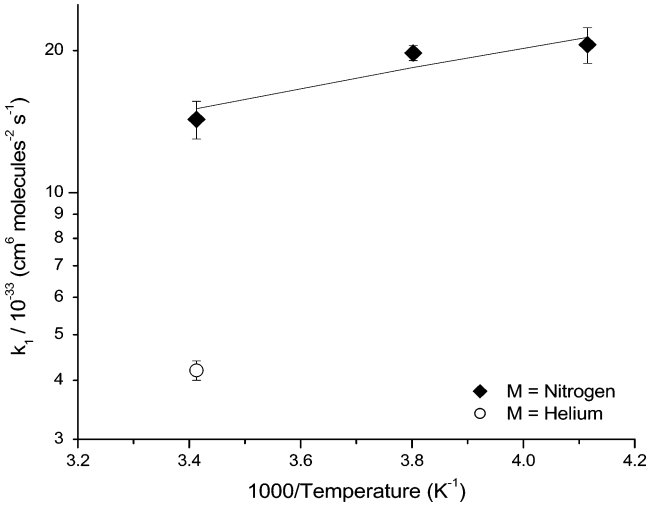

Figure 6. Arrhenius plot of the third-order rate coefficients for the recombination of Hg and Br atoms, k_1, in N_2 and He.

concentration was a critical component in measuring the rate coefficient for the mercury and bromine recombination reaction. The relative concentration profile was determined with good precision using LIF. However, the initial Br atom concentration was calculated and was, we believe, the largest source of systematic error in the reported rate coefficient for reaction 1. We can, however, make some assessment of the accuracy of this calculation by comparing our measured bromine atom recombination rate coefficients, which also depend on the accuracy of the calculation of the initial Br atom concentration, with literature values. As shown in Figure 3, bromine atom temporal profiles were monitored by LIF with the concentration typically followed to 5−20% of the initial bromine atom signal. Under each set of experimental conditions, i.e., a fixed pressure, temperature and initial bromine atom concentration, the effective second-order rate coefficient, k_2', for the recombination of Br atoms was calculated from the Br temporal profile using eq VIII,

$$\frac{1}{[\text{Br}]_t} = 2k_2't + \frac{1}{[\text{Br}]_0} \quad \text{(VIII)}$$

again assuming a negligible first-order loss due to reaction with impurities or diffusion. Linear fits of plots of 1/[Br] vs time give the effective second-order recombination rate coefficient, k_2'. Figure 7 shows a series of plots for the reciprocal of absolute bromine atom concentration versus time. This provides an indication of the precision of the data sets, which were obtained at the same temperature and pressure. Each plot should have the same slope independent of initial Br atom concentration. The data shown in Figure 7 were taken at 243 K in 400 Torr nitrogen buffer gas with initial Br atom concentrations ranging from 1.8×10^{16} to 3.8×10^{16}. The plots demonstrated good linearity and gave an average second-order recombination rate coefficient of $(1.08 \pm 0.17) \times 10^{-13}$ cm^3 $molecule^{-1}$ s^{-1} where the uncertainty is a 2σ error of precision. To ensure that the addition of mercury did not affect the observed Br atom decay, experiments were conducted in the presence and absence of mercury. The temporal profiles and derived rate coefficients were identical within the precision of the measurements. This was expected because the Hg concentration was at least 3 orders of magnitude smaller than the initial Br atom concentration. The values of the effective second-order rate coefficients together with 2σ errors are summarized in Table 3.

The third-order recombination rate coefficients were then determined from linear fits of the plot of second-order rate

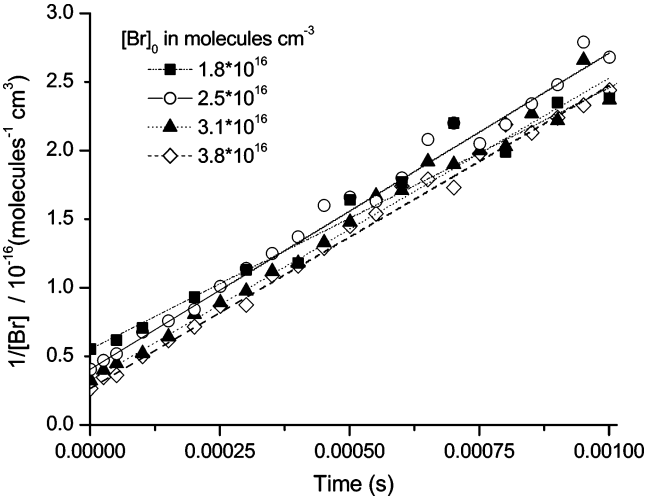

Figure 7. Second-order rate coefficient plot for Br atom, shown for measurements conducted in 400 Torr N_2 at 243 K.

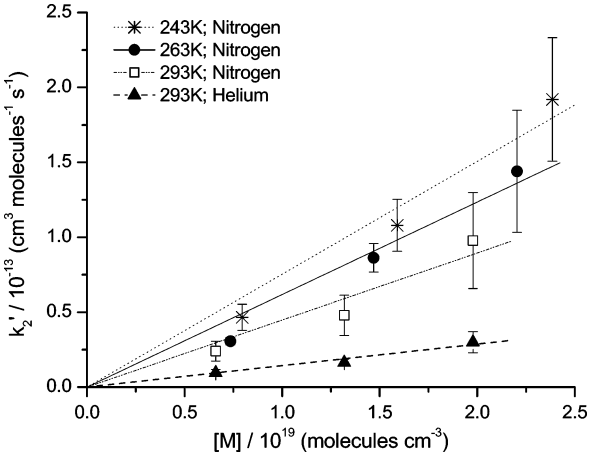

Figure 8. Variation of the effective second-order rate coefficients for the recombination of Br atoms, k_2', with pressure.

TABLE 3: Second-Order Rate Coefficients for the Recombination of Bromine Atoms, k_2'

gas	T (K)	P (Torr)	$10^{14}(k_1' \pm 2\sigma$ error) (cm^3 molecule^{-1} s^{-1})
N_2	243	200	4.66 ± 0.87
		400	10.8 ± 1.7
		600	19.2 ± 4.1
	263	200	3.06 ± 0.25
		400	8.63 ± 0.96
		600	14.4 ± 4.1
	293	200	2.44 ± 0.71
		400	4.80 ± 1.31
		600	9.71 ± 3.26
He	293	200	0.96 ± 0.22
		400	1.64 ± 0.22
		600	3.00 ± 0.70

coefficients, k_2', versus concentration of N_2 or He, as shown in Figure 8. As is the case for the Hg + Br recombination, the data show a good linear dependence of the effective second-order rate coefficient on pressure. However, we see a consistent, negative offset. As for reaction 1, the third-order rate coefficients were obtained by forcing all fits through the origin. The forced plots pass through most of the error bars associated with each data point whereas the difference in the slopes of the forced and unforced fits varied from 8% to 25%. The third-order recombination rate coefficients, k_2, are listed in Table 4 and plotted in Figure 9. For the data in nitrogen, the resulting

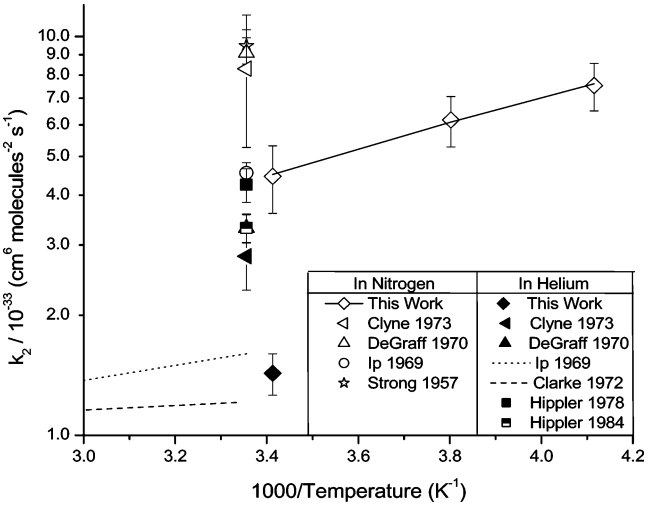

Figure 9. Arrhenius plot of the third-order rate coefficients for the recombination of Br atoms, k_2, in N_2 and He. Literature values are shown for comparison.

TABLE 4: Third-Order Rate Coefficients for the Recombination of Bromine Atoms, k_2, Determined in This Work at 293 K in He and 243, 263, and 293 K in N_2, with the Resulting Temperature Dependent Expression for N_2

gas	T (K)	$10^{33}(k_2 \pm 2\sigma$ error) (cm^6 molecule^{-2} s^{-1})
He	293	1.43 ± 0.17
N_2	243	7.53 ± 1.03
	263	6.18 ± 0.89
	293	4.46 ± 0.86
		$(4.31 \pm 0.21) \times 10^{-33} \times (T/298)^{-(2.77\pm0.30)}$

temperature dependent expression is given by

$$k_{2,N_2}(243-298\text{K}) = (4.31 \pm 0.21) \times 10^{-33} \times \left(\frac{T}{298}\right)^{-(2.77\pm0.30)} \quad \text{(IX)}$$

In eq IX the uncertainties are measures of 2σ error of precision only. As we discuss in detail below, we estimate an uncertainty of ±50% in the accuracy of the rate coefficient, due principally to the uncertainty in the calculation of absolute Br atom concentrations. Overall, the data showed the expected behavior for a three-body recombination, a positive pressure dependence, an inverse temperature dependence, and a higher deactivation efficiency for nitrogen relative to helium.

Potential Sources of Systematic Error. As we have noted above, the variation of the effective second-order rate coefficients with pressure should show a linear dependence that passes through the origin. In fact, the bromine atom recombination reaction data consistently show slight negative offset, which may be indicative of a systematic error in the calculation of the bromine atom concentration. It should be noted that these offsets were relatively small, and in most cases the fits that were forced through the origin passed within the 2σ errors of precision associated with each data point.

To calculate the initial bromine atom concentration, eq I was employed using the absorption cross-section of bromine molecules at 355 nm, the molecular bromine concentration, the average laser power, and the laser diameter. The error associated with the first two parameters in eq I should be less than 5%. As discussed previously, there is some uncertainty in the calculation of the effective diameter and homogeneity of the laser beam and hence the fluence. This was assessed by

TABLE 5: Comparison of Literature Data for Third-Order Rate Coefficients for the Recombination Bromine Atoms, k_2

gas	T (K)	P (Torr)	k_2 (cm^6 molecule^{-2} s^{-1})	ref
N_2	298	~500	$(9.46 \pm 0.94) \times 10^{-33}$	14
	300−1225	~100	$(4.55 \pm 0.55) \times 10^{-33}$ [a]	15
	298−373	2.2−3.2	$(9.1 \pm 0.83) \times 10^{-33}$	16
	298	~2.25	$(8.3 \pm 0.30) \times 10^{-33}$	18
	293	750−5250000	$(1.1 \pm 0.11) \times 10^{-32}$	19
	243−293	200−600	$(4.31 \pm 0.21) \times 10^{-33} \times (T/298)^{-(2.77\pm0.30)}$	this work
He	300−1225	100−300	$1.6 \times 10^{-33} \times (T/298)(-1.26 \pm 0.04)$ [a]	15
	298−373	2.2−3.2	$(3.31 \pm 0.27) \times 10^{-33}$	16
	300−1500	760	$1.725 \times 10^{-33} \times (T/298)^{-0.68} \times \exp(-0.21(\text{kcal/mol})/RT)$ [a]	17
	298	~2.25	$(2.81 \pm 0.50) \times 10^{-33}$	18
	293	750−5250000	$(4.25 \pm 0.41) \times 10^{-33}$	31
	293	750−5250000	$(3.31 \pm 0.78) \times 10^{-33}$	19
	293	200−600	$(1.43 \pm 0.17) \times 10^{-33}$	this work

[a] Rate coefficients were corrected to include factor of 2 for second-order rates.

measuring the variation in the fluence across the width of the beam. We estimate the error in the diameter determination to be less than 10%. However, the error associated with the calibration of the laser power meter, homogeneity within the beam profile, and shot to shot variability increase the uncertainty and result in an estimated error of ±20% in the fluence. Therefore, we believe that ±30% represents a conservative overall estimate of the uncertainty in the Br atom concentrations. A second source of systematic error could be the influence of secondary chemistry on the bromine atom temporal profiles. Molecular bromine does not thermally dissociate at the temperatures in this study. No experimental data are available for reactions of HgBr and we expect it to react with both Br and Br_2; however, its concentration is much lower than that of [Br] and it should not affect Br atom profiles. However, the fate of HgBr is a significant uncertainty in assessing the role of Br in AMDEs. Considering the typical errors of precision in the data and the possibility of other small, but unidentified, systematic errors, we believe that ±50% represents a reasonable estimate of the overall uncertainty in the measured rate coefficients.

Discussion and Comparison with Previous Work

Bromine Atom Recombination. The bromine atom recombination reaction, k_2, has been determined in both helium and nitrogen in several studies.[14−19,31] The results of these studies, including the specific pressure and temperature regimes used are outlined in Table 5. When evaluating these studies, it is essential to identify the relationship used to determine the rate coefficient. In the review of literature we found that three relationships were used to evaluate k_2, eqs IV, X, and XI.

$$\frac{d[Br_2]}{dt} = k_2[Br]^2[M] \quad \text{(X)}$$

$$\frac{d[Br]}{dt} = -k_2[Br]^2[M] \quad \text{(XI)}$$

Equations IV and X should result in an equivalent k_2 rate coefficient, whereas eq XI will result in an expression of the k_2 rate coefficient that is a factor of 2 too fast. Therefore, two studies[15,17] had to be corrected for this factor of 2 to be comparable to our second-order rate coefficients. Once corrected, these two rate coefficient agree, within error limits, with our rate determination for the Br atom self-reaction in both helium and nitrogen.

On the other hand the rates determined by Strong et al.,[14] DeGraff et al.,[16] Clyne et al.,[18] and Hippler et al.[19,31] are consistently a factor of 2−3 faster than our rate determination. All of these studies reported agreement with the earlier Ip et al. study,[15] without accounting for the difference of a factor of 2 in the defined second-order rate coefficient, when, in fact, the reported rate coefficients for the later studies are a factor of 2−3 faster than the Ip et al. study.

In assessing potential sources of systematic error, we can identify two possible complications in our experimental approach. The first is additional loss of bromine atoms by reaction with impurities. However, any additional reaction, which resulted in the loss of bromine atoms, would increase the observed rate. Because the rate that we observed is slower than that in the previous studies, this cannot account for the observed discrepancy. The second possible complication in our system is the over- or underestimation of the Br atom concentration. Because we must determine absolute Br atom concentrations, an error in this determination could affect the resulting rate coefficient. However, the errors associated with our determination were previously discussed and resulted in a maximum estimated error of ±30%; therefore this should not account for the discrepancy. We therefore agree with the earlier work of Ip et al.[15] and Clarke et al.[17]

Mercury and Bromine Atom Recombination. Three previous experimental[20−22] and two theoretical determinations[23,24] have reported values for reaction 1 and these results are compared with the current work in Table 6 and in Figure 10.

Greig et al.[20] used flash photolysis combined with absorption spectroscopy to study reaction 1 at temperatures 393−448 K in 200 Torr CF_3Br resulting in a rate coefficient of 2.82×10^{-13} cm^3 molecules^{-1} s^{-1}, with a reported error of a factor of 3. The rate coefficient obtained is not directly comparable to those reported here, due to temperature and buffer gas differences; however, using the temperature dependent expression reported in this work, we predict a recombination rate coefficient in 200 Torr nitrogen and 393 K of 5.7×10^{-14} cm^3 molecule^{-1} s^{-1}. This is approximately a factor of 4.5 slower than the rate coefficient reported by Greig et al. This difference in the rate coefficients might be explained by the difference in the third body efficiencies of CF_3Br versus N_2. Hippler et al. found C_3F_8 to be a factor of 6.5 more efficient as a third body than N_2 in a study of Br atom recombination.[19]

Additionally, we would identify two particularly significant sources of systematic error in the Greig et al. study. First, the system was a static system where a gas mixture undergoes repeated flashes. This experimental approach increases the possibility of secondary chemistry, product photolysis and interfering species. Second, to determine the rate coefficient for reaction 1 it was necessary to determine the absolute mercury bromide (HgBr) concentration. Mercury bromide concentrations

TABLE 6: Reported Rate Coefficients for the Recombination of Mercury and Bromine Atoms, k_1

gas	T (K)	P (Torr)	k_1	units for k_1	ref
N_2	298	760	$(3.2 \pm 0.3) \times 10^{-12}$	(cm^3 $molecule^{-1}$ s^{-1})	21
	298	760	3.0×10^{-13}	(cm^3 $molecule^{-1}$ s^{-1})	22
	298	760	9.7×10^{-13}	(cm^3 $molecule^{-1}$ s^{-1})	22
	298	760	1.01×10^{-12} exp(209.03/T)	(cm^3 $molecule^{-1}$ s^{-1})	23
	180−400	760	$1.1 \times 10^{-12} \times (T/298)^{-2.37}$	(cm^3 $molecule^{-1}$ s^{-1})	24
	243−293	760	$(1.46 \pm 0.34) \times 10^{-32} \times (T/298)^{-(1.86\pm1.49)}$	(cm^6 $molecule^{-2}$ s^{-1})	this work
He	243−293	760	$(4.2 \pm 0.2) \times 10^{-33}$	(cm^6 $molecule^{-2}$ s^{-1})	this work
CF_3Br	393−448	200	2.82×10^{-13}	(cm^3 $molecule^{-1}$ s^{-1})	20

were determined by monitoring the C_2F_6 concentration as a proxy for bromine atom concentrations and assuming that all the bromine atoms were converted to mercury bromide. The C_2F_6 was formed via the self-reaction of CF_3, a product of the flash photolysis of CF_3Br. By using C_2F_6 concentrations as a proxy for HgBr concentrations, the Grieg study assumes that all the Br atoms which were formed in the initial photolysis of the CF_3Br species, react with an Hg atom. Greig et al. assumed that the formation of mercury(II) bromide ($HgBr_2$) via reaction 4 was insignificant. However, if the rate coefficient calculated

$$HgBr + Br \rightarrow HgBr_2 \qquad (4)$$

by Goodsite et al.[24] for reaction 4 is correct, then reaction 4 could be a significant sink for bromine atoms. Thus the estimate of the [HgBr] could be too large, and this would result in the overestimation of the rate coefficient for reaction 1 in the Greig et al. determination.

Two more recent studies have utilized relative rate techniques to study reaction 1 at 1 atm and at room temperature. Ariya et al. reported rate coefficient for the reactions of Hg(0) with Cl_2, Cl, Br_2 and Br in a recent study.[21] We have discussed the rate coefficient obtained for the Hg(0) + Cl reaction previously.[25] In that case five different reference molecules were used, obtaining results that differed by a factor of 270 in the measured relative rates together with a strong nonlinearity of the relative rate plot when determined in a bath gas of air. Ultimately, a series of eight measurements were made using a single reference reaction, and the reported rate coefficient was determined from this small subset of the data. The rate coefficient that was obtained was a factor of 50 faster than the rate coefficient we obtained using a direct technique that was essentially identical to that reported here. We attributed the difference to presence of secondary chemistry in the relative rate system.

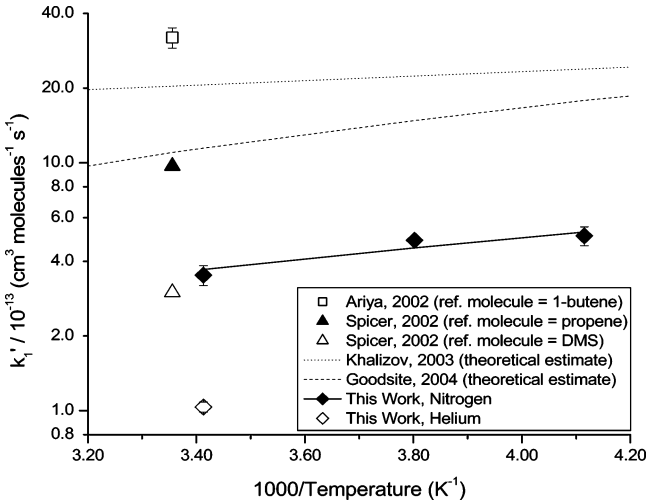

Figure 10. The second-order rate coefficients for the recombination of Hg and Br atoms, k_1 at 760 Torr, for this work in N_2 and He and literature values in N_2.

Ariya et al.[21] also reported a rate coefficient of $(3.2 \pm 0.3) \times 10^{-12}$ cm^3 $molecules^{-1}$ s^{-1} for reaction 1, which is a factor of 9 faster than the rate determined in this work. In contrast to their Cl atom work, Ariya et al. used a single reference reaction, Hg(0) with 1-butene, to measure the relative rate of reaction 1. Kinetic studies on the reaction of Hg(0) and 1-butene are limited, with only one study referenced.[32] Additionally, that study used a relative rate technique and noted that the observed rate coefficient depended on the O_2 partial pressure, indicating a complex reaction mechanism. In the Ariya et al. study the rate observed depended on the concentration of the reference molecule, the concentration of the OH scavenger, and the identity of the buffer gas. The observed reaction coefficient for reaction 1 varied by a factor of 3 as the buffer gas was varied between nitrogen and air. To obtain linear relative rate plots in the Ariya et al. study, they added large amounts of an OH scavenger (cyclohexane), leading to an enhancement in the absorption of reactant on the cell walls. Ariya et al. reported that the primary complication to their system was enhanced removal of the reference compound by reaction with OH or loss on the cell walls. Any additional loss of the reference compound would produce an underestimate of the rate coefficient. However, the rate coefficient obtained in that work exceeds both our directly measured rate coefficient and two theoretical estimates of the rate coefficient. We feel that a more plausible explanation would be additional loss of mercury, either by heterogeneous reaction or possibly by gas-phase reaction with an oxygenated species, because any additional process that removed mercury would generate the observed overestimate.

The second relative rate study, a technical report by Spicer et al.,[22] was performed in a 17.3 m^3 environmental chamber using two reference molecules dimethyl sulfide (DMS) and propene (C_3H_6) in a buffer gas of air. Spicer et al. reported values of 3.0×10^{-13} cm^3 $molecules^{-1}$ s^{-1} for the rate coefficient relative to DMS and 9.7×10^{-13} cm^3 $molecules^{-1}$ s^{-1} for the rate coefficient relative to propene. They gave greater weight to the higher value because the results obtained using the DMS reference were more variable. Again the factor of 3 variation of the measured relative rate on the identity of the reference compound implies that the measured rates were influenced by secondary or heterogeneous chemistry.

In addition to the experimental work described above, there have been two theoretical determinations of the rate coefficient. Khalizov et al.[23] determined the recombination rate coefficient for reaction 1 using electronic structure calculations to obtain both molecular parameters and the capture rate or high-pressure limit. Once this high pressure limit was obtained, Khalizov et al. determined a pressure dependent rate coefficient by assuming a strong collisional deactivation. To compare this with the observed data, it is essential to consider the mechanism of a three-body recombination. A three-body recombination consists of an initial collision that generates an excited complex, reaction 5. A portion of the excited complex will directly decompose back into reactants, reaction 6, whereas the other portion

undergoes a collision and is stabilized, reaction 7. The calculated

$$Hg + Br \rightarrow HgBr^* \quad (5)$$

$$HgBr^* \rightarrow Hg + Br \quad (6)$$

$$HgBr^* + M \rightarrow HgBr + M \quad (7)$$

pressure dependent rate coefficient reported by Khalizov et al. made the physically unrealistic assumption that every collision of the buffer gas with the initially formed energized HgBr* complex deactivated the complex to produce a stable HgBr molecule that cannot dissociate to products. If the initial calculation of the capture rate coefficient, reaction 5, is accurate, this assumption should produce the maximum possible recombination rate coefficient under each set of conditions. They obtained a rate coefficient of 2.07×10^{-12} cm^3 molecule^{-1} s^{-1} at 298 K, 760 Torr.

The second theoretical study of reaction 1 was carried out by Goodsite et al.[24] This study employed the RRKM theory using a master equation formulation to predict the rate coefficient for several mercury reactions of interest. In this work the rate of deactivation of HgBr* is calculated by assigning the energy of HgBr* into a series of energy grains and assuming that the average energy removed by each collision with N_2 was 400 cm^{-1}. The rate coefficient obtained using this approach was 1.1×10^{-12} cm^3 molecules^{-1} s^{-1}. This more physically realistic energy transfer model produces a rate coefficient that is a factor of 2 slower than the study of Khalizov et al. However, both studies reported rate coefficients that were slower than the experimental rate coefficient reported in the Ariya study. Goodsite et al. addressed the large discrepancy with the Ariya et al. measurement and found that to obtain the experimental rate coefficient, the bond energy in HgBr had to be increased by 30 kJ mol^{-1} over the current experimental data of 74.9 kJ mol^{-1}. Because the error limit of the experimental determination of the bond energy is only ± 4 kJ mol^{-1}, the authors concluded that the Ariya et al. rate coefficient was overestimated.

The determination of the reaction coefficient for reaction 1 at 298 K and 760 Torr of 3.6×10^{-13} cm^3 molecules^{-1} s^{-1} from this work reflects a rate coefficient that is a factor of 3 and factor of 6 slower than the two theoretical studies. As noted above, the strong collision assumption is normally physically unrealistic and should give an upper limit to the rate coefficient. Our results suggest that the 400 cm^{-1} energy removal parameter of Goodsite et al. is a little too large. Incorporation of a slightly smaller value would produce a result in good agreement with our experimental value.

We should note that this is the first study of reaction 1 that has systematically varied the temperature, pressure and buffer gas. As we note above, our observations are entirely consistent with the behavior expected for a three body recombination and our rate agrees well with the two theoretical determinations.

Conclusions

We have reported recombination rate coefficients for the reaction of mercury and bromine atoms, k_1, together with the self-reaction of bromine atoms, k_2. In both cases the rate coefficients show pressure and temperature dependencies, as well as third body deactivation efficiencies, which are consistent with a three-body recombination. For reaction 1, the recombination of bromine with mercury, we obtain rate coefficients that are slower than previously reported rate coefficients. The discrepancy observed between this work and the relative rate studies together with the variability in those studies questions the viability of using the relative rate method to determine kinetic rate coefficients for mercury halogen reactions. For reaction 2, the self-reaction of bromine atoms, we obtain results, which are in agreement with the early experimental determination of Ip et al.[15] and the theoretical determination of Clarke et al.[17] but are somewhat slower than more recent studies

To evaluate the importance of the recombination of elemental mercury and bromine atoms, an effective second-order rate coefficient of 4.6×10^{-13} cm^3 molecules^{-1} s^{-1} was calculated from the reported temperature dependent expression for Arctic conditions, 260 K and 760 Torr. Assuming a peak concentration[33] of bromine atoms of 10^7-10^8 cm^{-3} the lifetime of mercury due to bromine is between 2.5 days and 6 h. This means reaction 1 could play a significant role in AMDEs. However, the importance of the recombination of mercury and bromine atoms, reaction 1, will depend on the stability and reactivity of the HgBr species. Further studies into the reactivity of HgBr are ongoing.

Finally, Hedgecock et al.[13] reported a lifetime of mercury in the MBL of 10.5 days. This lifetime assumes that removal by reaction 1 is the dominant process in the conversion of elemental mercury to reactive gaseous mercury, with reaction with OH and ozone playing an important but lesser role. To calculate this lifetime, Hedgecock et al. assumed a steady-state Br concentration of [Br] $= 3.1 \times 10^5$ molecules cm^{-3} and used the rate coefficient reported by Ariya et al.,[21] this results in a lifetime of elemental mercury due to reaction with bromine atoms of 11.5 days. If we perform the same calculation using the rate coefficient for reaction 1 determined in this work at 760 Torr and 298 K, we find the lifetime of mercury due to the reaction with bromine increases to 104 days. Using the Hedgecock et al. lifetimes of 133 days for reaction with OH and 578 days for reaction with O_3, we obtain an overall lifetime of 53 days for mercury in the MBL. The factor of 5 increase in the lifetime of Hg(0) using our rate coefficient for reaction 1 highlights the need for direct determination of rate coefficients for Hg(0) reactions to elucidate the overall biogeochemical cycling of mercury.

Acknowledgment. This research has been supported by a grant from the U.S. Environmental Protection Agency's Science to Achieve Results (STAR) program. The clarity of the paper was improved by the comments of the two anonymous referees.

Note Added in Proof. In *Rate coefficient for gas-phase oxidation of elemental mercury by bromine and hydroxyl radicals.* Sommar, J.; Gårdfelt, K.; Feng, X.; Lindquist, O. Paper presented at the 5th International Conference on Mercury as a Global Pollutant, Rio de Janeiro, 1999, a value of $(2.8 \pm 0.8) \times 10^{-13}$ cm^3 molecule^{-1} s^{-1} was reported for the rate coefficient for reaction 1 using a relative rate technique.

References and Notes

(1) Lockhart, W. L.; Wilkinson, P.; Billeck, B. N.; Danell, R. A.; Hunt, R. V.; Brunskill, G. J.; Delaronde, J.; St Louis, V. *Biogeochemistry* **1998**, *40*, 163.

(2) Wagemann, R.; Innes, S.; Richard, P. R. *Sci. Total Environ.* **1996**, *186*, 41.

(3) Wheatley, B.; Wheatley, M. A. *Sci. Total Environ.* **2000**, *259*, 23.

(4) Schroeder, W. H.; Anlauf, K. G.; Barrie, L. A.; Lu, J. Y.; Steffen, A.; Schneeberger, D. R.; Berg, T. *Nature* **1998**, *394*, 331.

(5) Lindberg, S. E.; Brooks, S.; Lin, C. J.; Scott, K. J.; Landis, M. S.; Stevens, R. K.; Goodsite, M.; Richter, A. *Environ. Sci. Technol.* **2002**, *36*, 1245.

(6) Ebinghaus, R.; Kock, H. H.; Temme, C.; Einax, J. W.; Lowe, A. G.; Richter, A.; Burrows, J. P.; Schroeder, W. H. *Environ. Sci. Technol.* **2002**, *36*, 1238.

(7) Temme, C.; Einax, J. W.; Ebinghaus, R.; Schroeder, W. H. *Environ. Sci. Technol.* **2003**, *37*, 22.
(8) Skov, H.; Christensen, J. H.; Goodsite, M. E.; Heidam, N. Z.; Jensen, B.; Wahlin, P.; Geernaert, G. *Environ. Sci. Technol.* **2004**, *38*, 2373.
(9) Berg, T.; Bartnicki, J.; Munthe, J.; Lattila, H.; Hrehoruk, J.; Mazur, A. *Atmos. Environ.* **2001**, *35*, 2569.
(10) Barrie, L. A.; Bottenheim, J. W.; Schnell, R. C.; Crutzen, P. J.; Rasmussen, R. A. *Nature* **1988**, *334*, 138.
(11) Sander, R.; Vogt, R.; Harris, G. W.; Crutzen, P. J. *Tellus Ser. B−Chem. Phys. Meteorol.* **1997**, *49*, 522.
(12) Hedgecock, I. M.; Pirrone, N.; Sprovieri, F.; Pesenti, E. *Atmos. Environ.* **2003**, *37*, S41.
(13) Hedgecock, I. M.; Pirrone, N. *Environ. Sci. Technol.* **2004**, *38*, 69.
(14) Strong, R. L.; Chien, J. C. W.; Graf, P. E.; Willard, J. E. *J. Chem. Phys.* **1957**, *26*, 1287.
(15) Ip, J. K. K.; Burns, G. *J. Chem. Phys.* **1969**, *51*, 3414.
(16) DeGraff, B. A.; Lang, K. J. *J. Phys. Chem.* **1970**, *74*, 4181.
(17) Clarke, A. G.; Burns, G. *J. Chem. Phys.* **1972**, *56*, 4636.
(18) Clyne, M. A. A.; Woon-Fat, A. R. *J Chem. Soc., Faraday Trans. 2* **1973**, *69*, 412.
(19) Hippler, H.; Schubert, V.; Troe, J. *J. Chem. Phys.* **1984**, *81*, 3931.
(20) Greig, G.; Gunning, H. E.; Strausz, O. P. *J Chem. Phys.* **1970**, *52*, 3684.
(21) Ariya, P. A.; Khalizov, A.; Gidas, A. *J. Phys. Chem. A* **2002**, *106*, 7310.
(22) Spicer, C. W.; Satola, J.; Abbgy, A. A.; Plastridge, R. A.; Cowen, K. A. *Kinetics of Gas-Phase Elemental Mercury Reactions with Halogen Species, Ozone, and Nitrate Radical under Atmospheric Conditions*; Florida Department of Environmental Protection: 2002.
(23) Khalizov, A. F.; Viswanathan, B.; Larregaray, P.; Ariya, P. A. *J. Phys. Chem. A* **2003**, *107*, 6360.
(24) Goodsite, M. E.; Plane, J. M. C.; Skov, H. *Environ. Sci. Technol.* **2004**, *38*, 1772.
(25) Donohoue, D. L.; Bauer, D.; Hynes, A. J. *J. Phys. Chem. A* **2005**, *109*, 7732.
(26) Oldman, R. J.; Sander, R. K.; Wilson, K. R. *J. Chem. Phys.* **1975**, *63*, 4252.
(27) Maric, D.; Burrows, J. P.; Moortgat, G. K. *J. Photochem. Photobiol. A−Chem.* **1994**, *83*, 179.
(28) Rodgers, M. O.; Asai, K.; Davis, D. D. *Appl. Opt.* **1980**, *19*, 3597.
(29) Simeonsson, J. B.; Sausa, R. C. *Spectrochim. Acta Pt. B−At. Spectrosc.* **1994**, *49*, 1545.
(30) Braun, W.; Herron, J. T.; Kahaner, D. *ACUCHEM/ACUPLOT*; National Bureau of Standards: Gaithersburg, MD, 1986.
(31) Hippler, H.; Luu, S. H.; Teitelbaum, H.; Troe, J. *Int. J. Chem. Kinet.* **1978**, *10*, 155.
(32) Barnes, I.; Bastian, V.; Becker, K. H.; Overath, R.; Zhu, T. *Int. J. Chem. Kinet.* **1989**, *21*, 499.
(33) Boudries, H.; Bottenheim, J. W. *Geophys. Res. Lett.* **2000**, *27*, 517.